

## Experimental Breaking of an Adiabatic Invariant

J. Notte and J. Fajans

*Physics Department, University of California, Berkeley, California 94720*

R. Chu and J. S. Wurtele

*Physics Department and Plasma Fusion Center, Massachusetts Institute of Technology, Cambridge, Massachusetts 02139*

(Received 5 January 1993)

When a cylindrical pure electron plasma is displaced from the center of the trap, it performs a bulk circular orbital motion known as the  $l = 1$  diocotron mode. The slow application of a perturbing potential to a patch on the trap wall distorts the orbit into a noncircular closed path. Experiments and a simple theoretical model indicate that the area enclosed by the loop is an adiabatic invariant. Detailed studies are made of the breaking of the invariant when perturbations are rapidly applied. When the perturbation is applied with discontinuous time derivatives, the invariant breaking greatly exceeds the predictions of the standard theory for smooth perturbations.

PACS numbers: 52.25.Wz, 03.20.+i, 47.15.Ki, 52.20.Fs

Adiabatic invariants are widely used in the analysis of many classical systems, perhaps most notably in plasma physics [1,2]. The existence of these invariants has generally been established by theoretical analysis complemented by numerical simulations. Few detailed experimental studies of adiabatic invariants have been reported. Here we report an experimental study of diocotron mode dynamics in a pure electron plasma which shows that the area enclosed by the diocotron orbit is an adiabatic invariant and the amount by which the invariant is broken by perturbations is strongly dependent on the functional form by which the perturbations are ramped up. Adiabatic invariants are commonly defined for single particle motions. Since the diocotron mode results from collective, multiparticle interactions, our invariant exists for the plasma as a whole. Nonetheless, as far as the adiabatic invariant is concerned, the motion of the plasma column as a whole generally follows that of a single line charge.

Our pure electron plasma is confined in a standard non-neutral plasma trap; the plasma column is held within a conducting cylinder by a coaxial magnetic field (providing radial confinement) and by negative potentials applied at the cylinder ends (providing axial confinement) [3]. Motion of the plasma column is dominated by bounce averaged  $\mathbf{E} \times \mathbf{B}$  drifts. When displaced from the center of the trap, the plasma column induces an image charge on the confining cylinder wall. The resulting radial electric field produces an azimuthally directed  $\mathbf{E} \times \mathbf{B}$  drift, forcing the plasma column to trace a circular orbit (see Fig. 1). This motion is the well-studied  $l = 1$  diocotron mode [4-6]. Voltages applied to a previously grounded azimuthal patch (see Fig. 1) generate electrostatic perturbations which distort the shape of the orbit. We define  $A_\Phi$  to be the area enclosed by the orbit of the center of charge of the plasma, and we find that  $A_\Phi$  is an adiabatic invariant. As with any adiabatic invariant,  $A_\Phi$  remains constant if the perturbations are applied sufficiently slowly, even when the perturbations significantly deform the orbit. In contrast, rapidly applied perturbations change both  $A_\Phi$  and the shape of the orbit. (In this paper, the terms "slow" and "rapid" refer to the time scale over which the perturbation is applied compared with the diocotron period.) A Hamiltonian model illustrates why  $A_\Phi$  is an adiabatic invariant, and accurately predicts the experimental change in the adiabatic invariant for fast perturbations. In the limit that the electron plasma can be approximated by a line charge,  $A_\Phi$  reduces to the flux surface adiabatic invariant,  $\Phi$  [1].

The observed adiabatic invariant breaking is strongly dependent on how a given perturbation is applied. The important factors include: (1) the time scale over which the perturbation is applied, (2) the functional form by which the perturbation is ramped up to its final value, and (3) the phase of the orbit at the time the perturbation is applied. The standard textbook description [7-9] of adiabatic breaking is inappropriate for non-

The observed adiabatic invariant breaking is strongly dependent on how a given perturbation is applied. The important factors include: (1) the time scale over which the perturbation is applied, (2) the functional form by which the perturbation is ramped up to its final value, and (3) the phase of the orbit at the time the perturbation is applied. The standard textbook description [7-9] of adiabatic breaking is inappropriate for non-

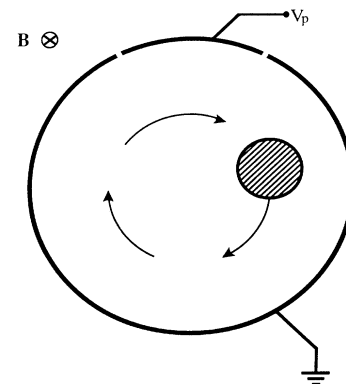


FIG. 1. An electron plasma column undergoing circular diocotron motion within the conducting cylinder. Axial confinement is provided by applying negative potentials to the ends of the cylinder (not shown).

0031-9007/93/70(25)/3900(4)\$06.00

© 1993 The American Physical Society

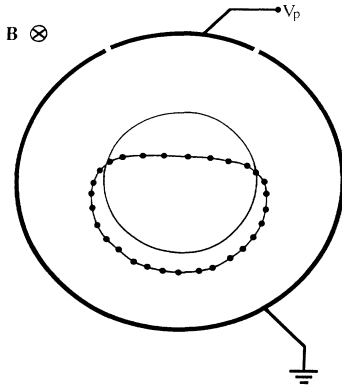


FIG. 2. A circular orbit and an orbit which has been distorted by the slow application of a  $V_p = 45$  V perturbation. The dots ( $\bullet$ ) represent the center of charge points from which the distorted orbit is determined.

analytically [10] ramped perturbations, and we believe that this is the first experimental observation of this phenomenon.

We perform the experiment with a repeated cycle of injection, manipulation, and analysis. During the injection phase, electrons from a hot tungsten filament are trapped within a grounded, conducting cylinder. During the manipulation phase, the electron column is first displaced from the cylinder center by growing an  $\ell = 1$  diocotron mode orbit to a known amplitude [5]. Next, the perturbation is applied by ramping the patch voltage from 0 to  $V_p$ , over a time scale  $T_r$ , by a chosen ramping function (such as a linear ramp or hyperbolic tangent ramp). At this point the previously circular orbit distorts into a non-circular closed loop. Finally, during the analysis phase, the shape of the orbit is ascertained. One of the negative confining voltages is momentarily grounded, allowing the electrons to rapidly dump out along the magnetic field lines and onto a phosphor screen. The resulting image is captured on a charge-coupled device camera and the center of charge is computed. This cycle is repeated 30 times; each time the plasma is dumped at a slightly different orbital position, thereby obtaining a set of points which defines the orbit. Typically, the electron column has radius  $r_p = 0.5$  cm, density  $n_p = 5 \times 10^7$  cm $^{-3}$ , temperature  $\approx 3$  eV, and length  $\approx 3$  cm. A typical diocotron orbit has an orbital area of  $A_\Phi \approx 1$  cm $^2$ , and a period of  $T_d = 10$   $\mu$ s. The wall patch subtends an angle of  $49.5^\circ$ , and has a length of 2.5 cm. The experimental procedures described here are common to pure electron plasma experiments; more explicit descriptions can be found in the literature [3,5,6].

Figure 2 shows both an unperturbed, circular diocotron orbit and a second orbit that has been distorted by a slow perturbation ( $T_r/T_d = 300$ ). When the perturbation is applied slowly, the area enclosed by the orbit,  $A_\Phi$ , is unchanged despite the fact that the orbit is distorted significantly. Figure 3 shows that  $A_\Phi$  is invariant

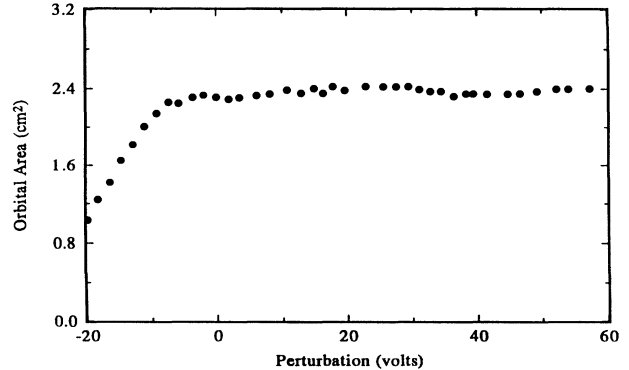


FIG. 3.  $A_\Phi$  vs  $V_p$ , when  $V_p$  is applied slowly ( $T_r/T_d = 300$ ).

for a wide range of slowly applied positive perturbations. Negative perturbations, however, reduce  $A_\Phi$  significantly. Such negative perturbations push the plasma so close to the cylindrical wall that some electrons are lost, thereby destroying the invariant.

The adiabatic invariant is broken by rapidly applying the perturbing voltage. We find that the change in the adiabatic invariant,  $\Delta A_\Phi$ , depends on three factors: the time scale taken to ramp the perturbation from ground to  $V_p$ , the functional form by which the perturbation is applied, and the angular position  $\theta$  of the plasma about the center of the trap when the perturbation is first applied. Figure 4 shows the phase dependence of  $\Delta A_\Phi$  using the linear ramping function for two different values of  $T_r/T_d$ . Note that the slower perturbation (by a factor of  $\sim 3$ ) produces an adiabatic breaking which is only slightly (by a factor of  $\sim 3$ ) less than the adiabatic breaking from the faster perturbation. This is in sharp contrast to the standard textbook analysis [7–9] which predicts an exponential decrease in amplitude. Note also that for each value of  $T_r/T_d$ , there exist values of  $\theta$  which produce a maximum increase and a maximum decrease in  $A_\Phi$ . Similar phase dependencies of adiabatic invariant breaking have been reported in theoretical, experimental, and numerical studies [11–13]. The existence of both signs of  $\Delta A_\Phi$  in Fig. 4 can be understood by considering the limit in which the perturbation is applied instantaneously. Without any perturbation, the allowed orbits are a set of concentric circles. Perturbations deform the orbits into a set of nested, noncircular, closed loops, each with a unique orbital area. If the perturbation is turned on instantly, the plasma then follows the noncircular orbit which intersects the circular orbit at the plasma's present position. This new orbit can enclose a greater or lesser area, depending upon the position of the plasma at the time the perturbation was applied.

Figure 5 shows the amount by which the invariant is broken as a function of the ramping time scale. For each value of  $T_r/T_d$ , a scan over  $\theta$  (similar to Fig. 4) gives both the largest positive and the largest negative deviations,  $\Delta A_\Phi$ . These maxima are plotted in Fig. 5 both for

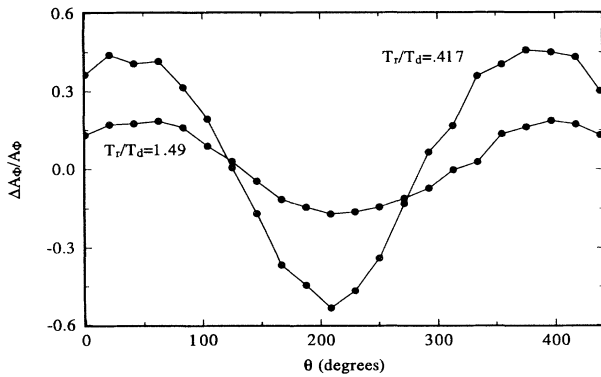


FIG. 4.  $\Delta A_\Phi/A_\Phi$  vs  $\theta$ , for  $V_p = 30$  V,  $A_\Phi = 1.05$  cm<sup>2</sup>, using the linear ramping function and for two values of  $T_r/T_d$ . The zero of the  $\theta$  axis is arbitrary.

a linear ramping function and for a hyperbolic tangent ramping function. The hyperbolic tangent ramping function produces an adiabatic breaking which falls off very rapidly to the noise level of these experiments. The falloff is found to be of the form  $\Delta A_\Phi \propto e^{-b(T_r/T_d)}$ , where a best fit in the exponential region indicates  $b = 3.1 \pm 0.2$ . This is the general form of adiabatic breaking as predicted by the standard theory.

The adiabatic breaking produced from the linear ramping function, however, is distinctly different. It consists of sinusoidlike oscillations bounded by a slowly decaying envelope (see Fig. 5). The period of the oscillation is  $T_d$  with the minima occurring at nearly integer values of  $T_r/T_d$ . The amplitude of the sinusoid envelope approaches zero according to the power law  $\Delta A_\Phi \propto (T_r/T_d)^N$ . The best fit for  $N$  gives  $N = -0.95 \pm 0.03$ . This power law is in sharp contrast with the exponential breaking law which was produced by the hyperbolic tangent ramp. A simple theoretical model [14], in which the cylindrical plasma is treated as a line charge, is in agreement with the experimental results. Figure 5 shows this excellent agreement for both the linear and hyperbolic tangent ramping functions.

Most theoretical treatments [7-9,11] of adiabatic breaking consider only perturbations which are ramped up analytically, usually with the hyperbolic tangent. Many experimental devices naturally implement analytic ramping functions, and in such cases the adiabatic breaking is found to be exponential [15,16]. Indeed, our adiabatic invariant  $A_\Phi$  is broken in this manner when the hyperbolic tangent is chosen as the ramping function. In general, however, the perturbation may be ramped from zero to its final value in a nonanalytic manner, as was done in this experiment using the linear ramp. While we are unaware of any previous experiments that report the results of a nonanalytic ramping, the theory of such ramps is discussed by Kulsrud [17] for harmonic oscillators. Kulsrud predicts that the adiabatic breaking should scale as  $(T_r/T_d)^{-(M+1)}$  for a ramping function which has

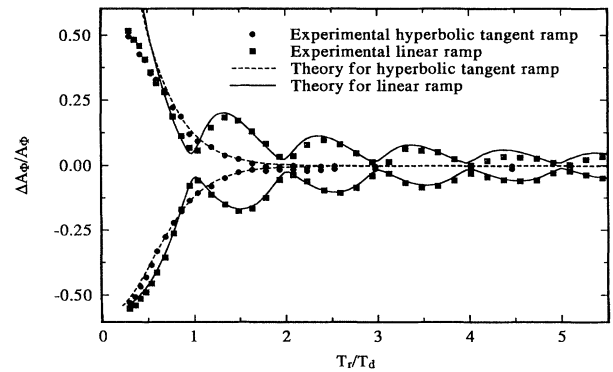


FIG. 5. Maximum and minimum  $\Delta A_\Phi/A_\Phi$  vs  $T_r/T_d$ , for  $V_p = 30$  V,  $A_\Phi = 1.05$  cm<sup>2</sup>, and two different ramping functions.

$M$  continuous derivatives. This is in excellent agreement with the experimental results of Fig. 5 (for a linear ramp,  $M = 0$ ). Kulsrud does not, however, predict the sinusoidal nature of Fig. 5. Recent simulations report a similar sinusoidal behavior when nonanalytic perturbations are used [13,14]. These simulations have also verified Kulsrud's scaling law for  $M = 0$  and 1, as well as for the hyperbolic tangent ramp.

It is straightforward to show that a perfectly circular plasma, independent of its size, follows the orbit of a single line charge [14]. However, our typical experimental plasma shape is actually somewhat elliptical and the applied perturbations cause the plasma shape to change throughout the course of its orbit. To study the effect of the plasma distortion on the center of charge orbit, we have developed a Hamiltonian which models the plasma as an ellipse with a changing aspect ratio and orientation. This elliptical plasma model shows that even a sizable change in the plasma shape and orientation has little effect on the plasma orbit, indicating that the energy change associated with such a variation can be offset by a very small change in the orbit [14]. Furthermore, we have shown analytically that a small plasma (like that used in the experiment), in general, is only slightly distorted by the applied perturbations. Hence, the plasma orbit can be accurately modeled by that of a single line charge. When the magnetic field,  $B$ , is constant, the Hamiltonian describing the  $\mathbf{E} \times \mathbf{B}$  drift dynamics is simply the electrostatic energy per unit length:

$$H(r, \theta) = \lambda \varphi_a(r, \theta, \epsilon t) + \lambda^2 \ln(1 - r^2/R_w^2), \quad (1)$$

where  $\lambda$  is the charge per unit length. Here, the first term is the energy of the line charge at the position  $(r, \theta)$  in the applied perturbing potential  $\varphi_a$ . The dependence of  $\varphi_a$  upon  $\epsilon t$  denotes the fact that  $\varphi_a$  is a slowly varying perturbation to the otherwise time-independent Hamiltonian. The second term is the interaction energy of the line charge with its image, where  $R_w$  is the cylindri-

cal wall radius. The momentum variable conjugate to  $\theta$  is  $P_\theta$ , where  $P_\theta = (B\lambda/2c)r^2$ . Hamiltonians with sufficiently slow perturbations have an adiabatic constant of the motion, namely, the integral of  $pdq$  over the phase space orbit [18]. This integral evaluates to

$$\oint P_\theta d\theta = \left(\frac{B\lambda}{c}\right) \int_0^{2\pi} \frac{r^2}{2} d\theta. \quad (2)$$

The remaining integral is the area of the orbit in polar coordinates, which is our definition of  $A_\Phi$ . Thus, for sufficiently slow perturbations, the area enclosed by the diocotron orbit is seen to be trivially proportional to the adiabatic invariant. The precise criteria for what constitutes a sufficiently slow perturbation is considered in depth by Kruskal [19]. This invariant,  $A_\Phi$ , is clearly analogous to the flux surface adiabatic invariant,  $\Phi$ , of plasma physics.

Although the above Hamiltonian [Eq. (1)] is exact only in the limit of a line charge or when the plasma column maintains a perfectly circular shape throughout its orbit, nevertheless, experiments with large radius, elliptical plasmas indicate that  $A_\Phi$  remains an adiabatic invariant.

In conclusion, we have discovered a new adiabatic invariant of the  $\ell = 1$  diocotron mode. We have measured the breaking of this invariant caused by rapid perturbations. Analytic perturbations break the adiabatic invariant in a manner which is predicted and observed in the literature. When we apply perturbations in nonanalytic fashion, we find that the change in the invariant is much larger than predicted by the standard textbook analysis. Experimentally, such nonanalytic perturbations are quite common. Examples for each of the three standard invariants include an electron beam propagating along the structured magnetic field of a magnetron injection gun ( $\mu$ ) [20], axial compression of a pure electron plasma ( $J_\parallel$ ) [21,22], and the effects of magnetic storms on the electrons in the Van Allen belt ( $\Phi$ ) [23]. In tokamaks, ions orbiting around fluctuations in the electrostatic potential have an adiabatic invariant which is analogous to  $\Phi$  [24].

The equations of motion which describe our system are isomorphic to the equations which govern the evolution of a two-dimensional inviscid, incompressible fluid [25]. Consequently, the results of this paper can also be generalized to vortex dynamics.

This work is supported by the Office of Naval Research, the National Science Foundation, and the Department of

Energy, Division of Nuclear and High Energy Physics.

- 
- [1] T. G. Northrop, *The Adiabatic Motion of Charged Particles* (Wiley Interscience, New York, 1963).
  - [2] D. R. Nicholson, *Introduction to Plasma Theory* (Wiley, New York, 1983).
  - [3] J. H. Malmberg *et al.*, in *Nonneutral Plasma Physics*, edited by C. Roberson and C. Driscoll, AIP Conf. Proc. No. 175 (American Institute of Physics, New York, 1988), p. 28.
  - [4] R. H. Levy, Phys. Fluids **8**, 1288 (1965).
  - [5] W. D. White, J. H. Malmberg, and C. F. Driscoll, Phys. Rev. Lett. **49**, 1822 (1982).
  - [6] K. S. Fine, C. F. Driscoll, and J. H. Malmberg, Phys. Rev. Lett. **63**, 2232 (1989).
  - [7] S. Chandrasekhar, *Plasma Physics* (University of Chicago Press, Chicago, 1965), p. 56.
  - [8] H. Goldstein, *Classical Mechanics* (Addison-Wesley, Menlo Park, 1980), 2nd ed., p. 538.
  - [9] A. J. Lichtenberg and M. A. Lieberman, *Regular and Stochastic Motion* (Springer-Verlag, New York, 1983), p. 86.
  - [10] By nonanalytic we mean that the ramping function has discontinuous time derivatives on the time scale of the orbital period or faster.
  - [11] J. E. Howard, Phys. Fluids **13**, 2407 (1970).
  - [12] R. H. Cohen, G. Rowlands, and J. H. Foote, Phys. Fluids **21**, 627 (1978).
  - [13] J. E. Borovsky and P. J. Hansen, Phys. Rev. A **43**, 5605 (1991).
  - [14] R. Chu *et al.*, Phys. Fluids B (to be published).
  - [15] A. Dubinina, L. Krasitskaya, and Y. Yudin, Plasma Phys. **11**, 551 (1969).
  - [16] J. Foote, Plasma Phys. **14**, 543 (1972).
  - [17] R. M. Kulsrud, Phys. Rev. **106**, 205 (1957).
  - [18] A. J. Lichtenberg and M. A. Lieberman, *Regular and Stochastic Motion* (Springer-Verlag, New York, 1983), p. 16.
  - [19] M. D. Kruskal, J. Math. Phys. **3**, 806 (1962).
  - [20] W. Lawson, IEEE Trans. Plasma Sci. **16**, 290 (1988).
  - [21] A. W. Hyatt, C. F. Driscoll, and J. H. Malmberg, Phys. Rev. Lett. **59**, 2975 (1987).
  - [22] B. R. Beck, J. Fajans, and J. H. Malmberg, Phys. Rev. Lett. **68**, 317 (1992).
  - [23] J. A. Sauvaud *et al.*, J. Geophys. Res. **92**, 2365 (1987).
  - [24] P. M. Bellan, Plasma Phys. Controlled Fusion **35**, 169 (1993).
  - [25] C. F. Driscoll and K. S. Fine, Phys. Fluids B **2**, 1359 (1990).